ELSEVIER

Journal of Nuclear Materials 258–263 (1998) 1193–1198

journal of nuclear materials

Effect of purity on helium bubble formation in 9Cr martensitic steel during post-implantation annealing at 1105 K

T. Nagasaka [a,*], T. Shibayama [b,1], H. Kayano [c,2], A. Hasegawa [d], M. Satou [d], K. Abe [d]

[a] *Graduate School of Engineering, Tohoku University, Aoba-ku, Sendai 980-8579, Japan*
[b] *The Oarai Branch, Institute for Materials Research, Tohoku University, Oarai-machi, Ibaraki 311-1313, Japan*
[c] *Tohoku University, Aramaki-aza-Aoba 01, Aoba-ku, Sendai 980-8579, Japan*
[d] *Department of Quantum Science and Energy Engineering, Tohoku University, Aramaki-aza-Aoba 01, Aoba-ku, Sendai 980-8579, Japan*

Abstract

Purification is essential to development of low-activation ferritic–martensitic steels for fusion reactor materials, not only from the practical viewpoint of reducing highly radioactive elements but also from the fundamental viewpoint of irradiation effects in ferritic steels and Fe–Cr alloys. A high-purity 9Cr–0.1C martensitic steel was prepared from an ultra-high-purity iron and high-purity alloying elements. In order to study the effect of large amount of helium on microstructure in the high-purity martensitic steel, 1000 appm of helium ions were implanted into the steel, and then TEM observation was performed after post-implantation annealing. It was observed that small cavities were distributed more densely in the high-purity steel than in commercial-grade ones. Moreover, the denuded zone near grain boundaries in the high-purity steel was much thinner than that in commercial-grade ones. The difference in cavity formation between the high-purity and commercial-grade steels is discussed.

1. Introduction

Ferritic–martensitic steels have been considered as promising candidate structural materials for fusion reactor applications because of their excellent swelling resistance, high thermal conductivity and low thermal expansion coefficient compared with austenitic steels. In these steels, reduced-activation martensitic steels with 8–9% Cr are the most attractive because of their relatively strong resistance to neutron irradiation embrittlement [1].

The purification of ferritic steels is essential from the viewpoint of reduction of activation. In order to reduce the nuclear waste and to lower the exposure of radiation, low-activation ferritic steels have been developed by use of elements which have low nuclear reaction cross section or short half-life. Also, the steels have to be purified to eliminate highly radioactive impurity elements. Permissible concentrations of Nb, Co and Ag, for example, according to 'hands-on' limit are 0.18, 1.7 and 0.011 wppm, respectively. No less than 20 elements have to be restricted below 10 wppm [2].

The recent success of production of ultra-high-purity iron, such as ultra-high-purity electrolytic iron [3] and FZ-iron refined by floating-zone (FZ) refining, led to the aspect that some properties of iron were not intrinsic but were the effect of impurities [4]. Several investigations of radiation effect on high-purity Fe–Cr alloys, prepared from the ultra-high-purity iron, have reported dislocation loop formation behavior through electron irradiation [5,6], tensile property change after neutron irradiation [7] and cavity formation after helium

* Corresponding author. Present address: National Institute for Fusion Science, Oroshi-cho, Toki, Gifu 509-5292, Japan. Tel.: +81-572 58 2137; fax: +81-572 58 2616; e-mail: nagasaka@nifs.ac.jp

[1] Present address: Center for Advanced Research on Energy Technology, Hokkaido University, Kita 13, Nishi 8, Kita-ku, Sapporo 060, Japan.

[2] Professor Emeritus.

0022-3115/98/$19.00
PII: S0022-3115(98)00185-8

implantation [8,9]. However, radiation effect on highly refined martensitic steels which will be utilized practically in the fusion reactor have not been studied yet.

Large amount of helium will be produced in fusion environment by transmutation, and was estimated to be 100 appm per 1 MW y m^{-2} [10] in ferritic steels. At the end of service life above 1000 appm helium will be accumulated in ferritic steels. Since the microstructural evolution may depend on helium content, the swelling and embrittlement behavior of ferritic steels under the existence of large amount of helium must be studied.

In this study, a high-purity Fe–9Cr–0.1C martensitic steel prepared from FZ-iron was used. The purpose of this paper is to study the effects of large amount helium on microstructural evolution in the high-purity martensitic steel, and to compare the results to those in commercial-grade ones.

2. Experimental procedure

An ultra-high-purity iron named FZ-iron was prepared from commercial high-purity electrolytic iron (99.99% nominal purity) by electron-beam melting in a vacuum of 10^{-4} Pa and FZ refining in flowing purified hydrogen atmosphere. A commercial high-purity chromium (99.99% nominal purity) and a spectroscopic-grade graphite were added into the FZ-iron or a commercial electrolytic iron (99.9% nominal purity) by arc-melting in a high-purity argon (99.9999% nominal purity) atmosphere; then buttons of both the high-purity and commercial-grade Fe–9Cr–0.1C alloys were obtained. The arc-melted buttons were hot-forged and cold-rolled in air into 0.5 mm thick sheets. TEM disks of 3 mm in diameter were punched out from the sheets. The punched disks and sheets were annealed at 1295 K for 1.8 ks and air-cooled, followed by tempering at 1033 K for 3.6 ks and air-cooling. The structure of all the steels was the single phase of tempered martensite. Table 1 shows the results of chemical analysis of the punched and heat-treated sheets. The high-purity alloy, FZ–Fe–9Cr–0.10C, contains almost 100% of additional carbon; however in the commercial-grade alloy named C-grade-Fe–9Cr–0.06C, only about 60% is remains. The rest, i.e. 40%, would react with oxygen in the commercial-grade iron and be released as CO gas, therefore the purity

Table 1
Chemical compositions in wppm of high-purity and commercial-grade 9Cr martensitic steels. Underlined elements were contained in both commercial-grade steels by above 10 times compared with high-purity one

Element	FZ-Fe–9Cr–0.10C	C-grade-Fe–9Cr–0.06C	C-grade-Fe–9Cr–0.15C
Cr	9.04 [a]	9.01 [a]	9.01 [a]
C	0.10 [a]	0.056 [a]	0.15 [a]
B	<0.05	<0.05	<0.05
H	1.1	0.9	3.4
N	42	106	39
O	2	6	6
P	0.3	7.9	7.8
S	3.3	50	52
Si	8	12	7
Al	0.4	23	20
Ag	<0.01	<0.01	<0.1
Bi	<0.1	<0.1	<0.1
Cd	<0.001	<0.001	<0.001
Co	<0.1	23	23
Cu	1.3	2.2	2.9
Hf	<0.2	0.2	<0.2
Mg	<0.01	<0.01	0.07
Mn	0.05	12	11
Mo	<0.2	0.8	1.0
Nb	<0.3	0.5	0.3
Ni	0.3	81	82
Pb	<0.01	<0.01	0.3
Ti	0.6	0.6	0.4
V	0.05	0.08	0.57
W	32	7	1
Zn	<0.1	<0.1	0.4
Zr	<0.1	<0.1	0.3

[a] Concentration in wt%.

effect can hardly be detected because of the difference in concentration of carbon. In order to study carbon effect in commercial-grade steel, the second steel called C-grade-Fe–9Cr–0.15C was prepared. In Table 1 underlined elements are the main impurities, such as phosphorus, sulfur, aluminum, cobalt, manganese and nickel which were contained in C-grade-Fe–9Cr–0.06C and C-grade-Fe–9Cr–0.15C more than 10 times compared with FZ-Fe–9Cr–0.10C. C-grade-Fe–9Cr–0.06C and C-grade-Fe–9Cr–0.15C successfully simulate the impurity levels of the conventional ferritic steels for fusion reactor materials [11].

Into the TEM disks 3 MeV ^{4}He ions were implanted at 293–313 K using Dynamitron accelerator with energy degrader and a beam monitor material at FNL (Fast Neutron Laboratory), Tohoku University. Calculation by TRIM-code [12] indicated that homogeneously implanted layer of 2.7 μm in thickness existed between 0.8 and 3.5 μm in depth from the implanted surface. The total amount of helium in this layer and associated displacement were estimated to be approximately 1000 appm and 0.2 dpa. After helium implantation TEM disks were annealed at 1105 K for 3.6 ks in a vacuum, followed by air-cooling. Then, TEM observation was performed on JEOL-2000FX (200kV) in the Oarai Branch, IMR (Institute for Materials Research), Tohoku University after sectioning and back-thinning.

3. Results

Fig. 1 shows microstructures of the 9Cr martensitic steels after post-implantation (1000 appm) annealing at 1105 K. Magnified images around the straight part of lath boundaries in Fig. 1(a) are shown in Fig. 1(b). In all the steels, cavities considered as helium bubbles were observed. As clearly shown in Fig. 1(b), smaller cavities were distributed in FZ-Fe–9Cr–0.10C compared with C-grade-Fe–9Cr–0.06C and C-grade-Fe–9Cr–0.15C. In C-grade-Fe–9Cr–0.06C and C-grade-Fe–9Cr–0.15C the denuded zone of about 50 nm in thickness from lath boundary occurred, while in FZ-Fe–9Cr–0.10C the one was below 10 nm thick or not observed. The aligned arrangement of the cavities which would be trapped by

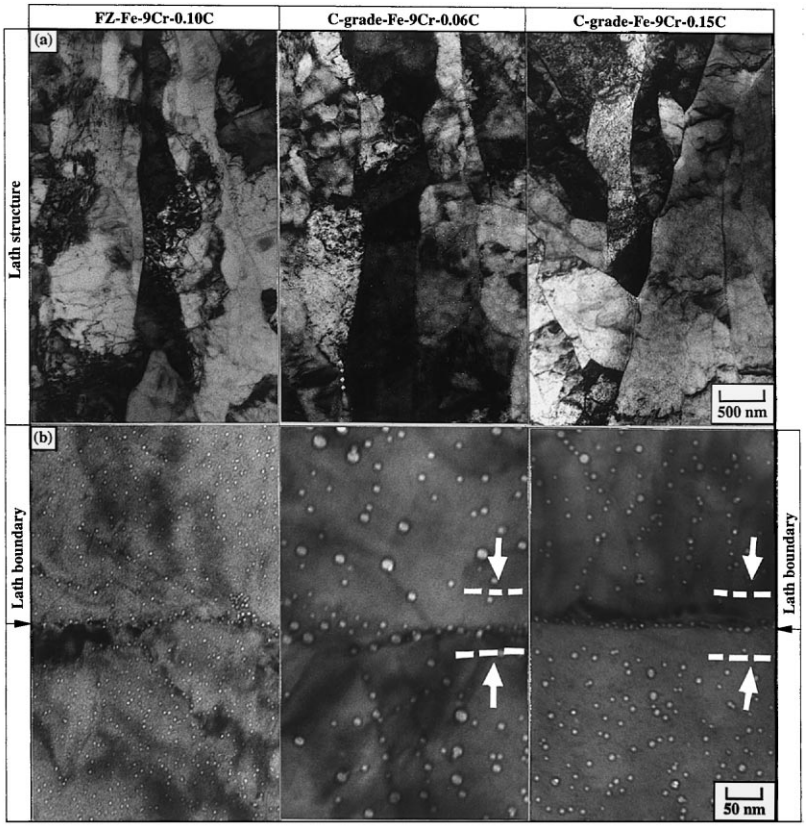

Fig. 1. TEM microstructure (a) of lath structure and (b) around lath boundary in 9Cr martensitic steels after implantation of 1000 appm helium and post-irradiation annealing at 1105 K for 3.6 ks. White arrows and dashed lines indicate denuded zone around lath boundary.

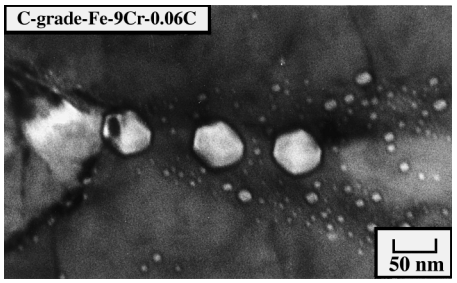

Fig. 2. Large cavities at the intersection of grain boundaries in commercial-grade 9Cr–0.06C martensitic steel.

dislocation was observed. In C-grade-Fe–9Cr–0.06C and C-grade-Fe–9Cr–0.15C relatively large denuded zone are observed around the dislocation too. In all the steels cavities were observed at grain boundary. Especially large cavities were observed at the intersection of grain boundaries in C-grade-Fe–9Cr–0.06C as shown in Fig. 2.

Fig. 3 shows histograms of size distribution of cavities inside the grain far enough from grain boundaries. In FZ-Fe–9Cr–0.10C a peak was observed at 4–6 nm, whereas in C-grade-Fe–9Cr–0.06C and C-grade-Fe–9Cr–0.15C that was at 6–8 nm. Almost all the cavities in FZ-Fe–9Cr–0.10C were in the range of 2–6 nm, while in C-grade-Fe–9Cr–0.06C the cavities below 4 nm were less observed, and the cavity size ranged upto about 20 nm. In C-grade-Fe–9Cr–0.15C the cavities of 2–4 nm were more preferential compared with those in C-grade-Fe–9Cr–0.06C, and the size distribution had a tendency to be shifted toward smaller size.

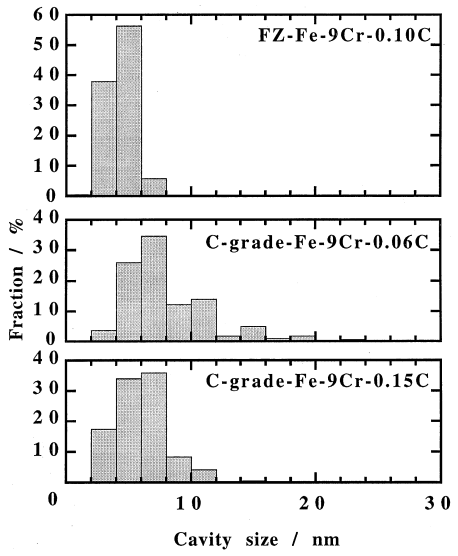

Fig. 3. Histograms of size distribution of cavity in 9Cr martensitic steels.

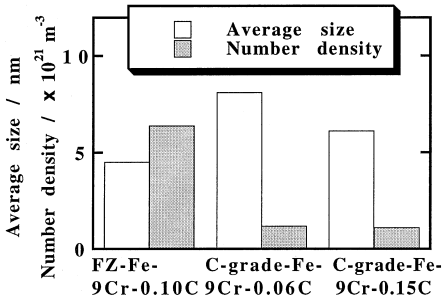

Fig. 4. Average size and number density of cavity.

Fig. 4 shows average size and number density of cavity inside the grain. The average size in FZ-Fe–9Cr–0.10C, C-grade-Fe–9Cr–0.06C and C-grade-Fe–9Cr–0.15C was 4.5 ± 0.6, 8.1 ± 1.0 and 6.1 ± 0.8 nm, whereas the number density was $6.4 \pm 4.0 \times 10^{21}$, $1.2 \pm 0.8 \times 10^{21}$ and $1.1 \pm 1.0 \times 10^{21}$ m^{-3}, respectively. In FZ-Fe–9Cr–0.10C small cavities were distributed more densely compared with those in C-grade-Fe–9Cr–0.06C and C-grade-Fe–9Cr–0.15C.

4. Discussion

4.1. Concentrations of highly radioactive elements

For example, both C-grade-Fe–9Cr–0.06C and C-grade-Fe–9Cr–0.15C contained about 20 wppm cobalt, which was harmful for low-activation materials, while in FZ-Fe–9Cr–0.10C the concentration of cobalt was less than 0.1 wppm. Though the detection limit of only niobium was not low enough, in FZ-Fe–9Cr–0.10C the amount of highly radioactive elements was successfully reduced and satisfied the requisite from 'hands-on' limit. Therefore, FZ-Fe–9Cr–0.10C can be a base material for low-activation ferritic steels.

4.2. Size and number density of cavities inside the grain

From the above results it was clear that smaller cavities were distributed more densely in the high-purity 9Cr martensitic steel compared with those in the commercial-grade ones. In the previous study using Fe–13Cr–0.1C steel, in situ TEM observation have clarified that cavity nucleation was practically completed within 1.5 ks during annealing at 873 K after helium implantation of 7700 appm [13]. After the nucleation stage relatively slow migration of cavities was observed, but several coalescences took place at 1123 K for 10.8 ks [14], which was 3 times longer than that in this study. When the FZ-Fe–9Cr–0.10C was annealed under the annealing temperature, 1105 K, cavities were too small to observe. The annealing temperature was higher than

the temperature utilized in the fusion reactor, but the annealing may make it possible to compare the number density of the pre-existing nucleation sites which were produced at the quenching and the tempering, during the implantation, or until the early stage of the annealing. TEM microstructures shown in Fig. 1 would indicate the distribution of the cavities after the nucleation stage and may reflect the number density of the nucleation site. FZ-Fe–9Cr–0.10C would have more nucleation sites for cavities inside the grain compared with C-grade-Fe–9Cr–0.06C and C-grade-Fe–9Cr–0.15C. In similar experiments on high-purity Fe–9Cr binary alloys, small cavities were distributed more densely in high-purity alloys compared with in commercial-grade ones [8]. It was due to sulfur addition of 50 wppm to high-purity Fe–9Cr alloy that cavities grew large [9]. Moreover, possibility of further growth caused by interaction between manganese and sulfur was suggested [9]. In this study C-grade-Fe–9Cr–0.06C and C-grade-Fe–9Cr–0.15C contain 50 and 52 wppm sulfur, respectively. In the commercial-grade steels sulfide clusters, such as FeS, CrS, MnS or their complex, may be produced because of segregation. The clusters may increase the concentration of vacancy around them by strong expansion strain field and act as nucleation sites for cavities. On the contrary, addition of interstitial solid solution, such as nitrogen, increased cavity number density [9], therefore solute carbon and nitrogen mainly become the nucleation site for cavities because of their strong strain field. The sulfide cluster, which was accompanied by segregation, would distribute more dilute and produce stronger strain field compared with the interstitial solute atoms, and this may be the cause of relatively dilute distribution of large cavities in C-grade-Fe–9Cr–0.06C and C-grade-Fe–9Cr–0.15C. Whereas, it may be caused by solute carbon that the fraction of small cavities in C-grade-Fe–9Cr–0.15C was larger than that in C-grade-Fe–9Cr–0.06C.

4.3. Cavity size and denuded zone at grain boundary

In C-grade-Fe–9Cr–0.06C and C-grade-Fe–9Cr–0.15C, a large denuded zone was observed in the vicinity of grain boundary and dislocation compared with that in FZ-Fe–9Cr–0.10C. It has been reported that sulfur addition increases cavity size at the grain boundary region [9]. On the other hand, using high-purity iron and Fe–S alloy, segregation of sulfur has been confirmed at grain boundary, when the sulfur content was above several 10 wppm [15]. The clusters containing sulfur may exist at grain boundary and dislocation as suggested above. The clusters would be aligned in one direction at a dislocation or located on grain boundary, which might produce the denuded zone. On the assumption that the inverse of the number density of cavity is equal to the volume of the sphere in which cavities can trap the helium atoms, migration distances of helium atoms in rough estimation are 33, 58 and 60 nm in FZ-Fe–9Cr–0.10C, C-grade-Fe–9Cr–0.06C and C-grade-Fe–9Cr–0.15C, respectively. This means that the denuded zone is two times thicker in C-grade-Fe–9Cr–0.06C and C-grade-Fe–9Cr–0.15C than in FZ-Fe–9Cr–0.10C. Contrary to the calculation, the denuded zone was very thin in FZ-Fe–9Cr–0.10C. On the other hand, cavity size at the grain boundary in C-grade-Fe–9Cr–0.15C was smaller than that in C-grade-Fe–9Cr–0.06C. These two results indicate that carbon atoms are concentrated on/around the grain boundary and dislocation and enhance nucleation of cavity.

4.4. Large cavity at the intersection of grain boundaries

The large cavities observed at the intersection of grain boundaries in C-grade-Fe–9Cr–0.06C may lead to a degradation of creep properties at elevated temperature. In austenitic steels, for example, cavity size of 12–20 nm was obtained as the critical value for degradation of creep rupture time at 1073 K [16]. On the other hand, the cavity size at the grain boundary in C-grade-Fe–9Cr–0.15C was rather smaller than that inside the grain. However, the total amount of helium would be larger than that in FZ-Fe–9Cr–0.10C because the denuded zone was formed. In FZ-Fe–9Cr–0.10C interstitial solute, such as carbon and nitrogen, may effectively act as nucleation site and decrease the amount of helium at grain boundary.

4.5. Cavity swelling

Fig. 5 shows cavity swelling calculated by the size distribution and the number density of cavities inside the grain. It was assumed that all cavities were spherical. The amount of swelling by cavities in all the steels was less than 0.1%. The cavity swellings in FZ-Fe–9Cr–0.10C and C-grade-Fe–9Cr–0.15C was relatively small. We cannot discuss about the difference of the swellings among the steels because the error of the swellings from

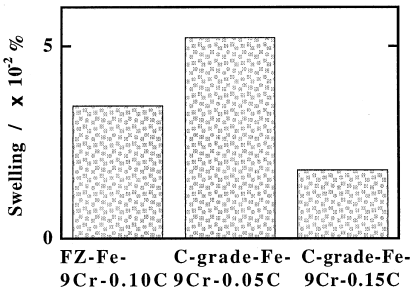

Fig. 5. Cavity swelling calculated by size distribution and number density of cavity.

the error of measurement of cavity size and number density is about 90%.

In fusion environment, cavities would be formed at temperatures lower than the annealing temperature, and at higher displacement damage. While more investigation should be conducted under higher displacement damage rate, this investigation indicates the possibility that the high-purity martensitic steels are quite different from the commercial-grade ones under the existence of relatively large amount of helium. From the view point of microstructural evolution, the purification might cause no degradation of the resistance to helium embrittlement and to cavity swelling in martensitic steels even under high production rate of helium.

5. Conclusions

The effect of purity on helium cavity formation in Fe–9Cr–0.1C martensitic steel was investigated using a high-purity low-activation steel after post-helium implantation annealing at 1105 K. The following results are obtained.

1. Small cavities were distributed more densely inside the grain in the high-purity steel compared with those in commercial-grade ones.
2. The width of the cavity denuded zone and the cavity size at the grain boundary in the high-purity steel was much smaller than that in commercial-grade ones.
3. In the high-purity steel, prepared from the FZ-refined iron, the amount of cavity swelling was less than 0.1%.

Acknowledgements

The authors are grateful to K. Sasaki and T. Sugawara of Core Laboratory of Crystal Science in IMR for preparing the ultra-high-purity iron, and to K. Takada and staff of the analysis team in IMR for chemical analysis, and to R. Sakamoto and M. Fujisawa of FNL for irradiation experiments. This work was supported by JUPITER program (Japan-USA Program of Irradiation Test for Fusion Research).

References

[1] A. Kohyama, A. Hishinuma, D.S. Gelles, R.L. Klueh, W. Dietz, K. Ehrlich, J. Nucl. Mater. 233–237 (1996) 138.
[2] G.J. Butterworth, S.R. Keown, J. Nucl. Mater. 186 (1992) 283.
[3] K. Abiko, in: K. Abiko, K. Hirokawa, S. Takaki (Eds.), Proceedings of the Conference on Ultra-High-Purity Base Metals (UHPM-94), Sendai, 1995, p. 1.
[4] T. Tabata, H. Fujita, H. Ishii, K. Igaki, M. Isshiki, Scripta Metal. 14 (1981) 1317.
[5] N. Yoshida, A. Yamaguchi, T. Muroga, Y. Miyamoto, K. Kitajima, J. Nucl. Mater. 155–157 (1988) 1232.
[6] E. Wakai, A. Hishinuma, Y. Kato, H. Yano, S. Takaki, K. Abiko, J. Physique (IV) 5 (1995) C7–277.
[7] E. Wakai, A. Hishinuma, T. Sawai, S. Kato, S. Isozaki, S. Takaki, K. Abiko, Phys. Status Solidi (A) 160 (1997) 285.
[8] T. Nagasaka, T. Shibayama, H. Kayano, A. Hasegawa, K. Abe, Sci. Rep. RITU A 45 (1997) 121.
[9] T. Nagasaka, T. Shibayama, H. Kayano, A. Hasegawa, K. Abe, to be published in Phys. Status Solidi (A) 167 (2).
[10] G.J. Butterworth, O.N. Jarvis, J. Nucl. Mater. 122–123 (1984) 982.
[11] D.S. Gelles, J. Nucl. Mater. 239 (1996) 99.
[12] J.F. Ziegler, J.P. Biersack, U. Littmark, The Stopping and Range of Ions in Solids, Pergamon Press, London, 1985.
[13] G. von Bradsky, P.J. Goodhew, J. Nucl. Mater. 135 (1985) 269.
[14] Z.H. Luklinska, G. von Bradsky, P.J. Goodhew, J. Nucl. Mater. 135 (1985) 206.
[15] C.M. Liu, T. Iyama, H. Suenaga, K. Abiko, M. Tanino, in: K. Abiko, K. Hirokawa, S. Takaki (Eds.), Proceedings of the Conference on Ultra-High-Purity Base Metals (UHPM-94), Sendai, 1995, p. 500.
[16] H. Ullmaier, J. Nucl. Mater. 133–134 (1985) 100.